

# Formation of $\eta^2$ C–H Agostic Rhodium Arene Complexes and Their Relevance to Electrophilic Bond Activation

Arkadi Vigalok,<sup>†</sup> Olivier Uzan,<sup>†</sup> Linda J. W. Shimon,<sup>‡</sup> Yehoshua Ben-David,<sup>†</sup>  
Jan M. L. Martin,<sup>\*,†</sup> and David Milstein<sup>\*,†</sup>

Contribution from the Departments of Organic Chemistry and Chemical Services, The Weizmann Institute of Science, Rehovot 76100, Israel

Received July 17, 1998

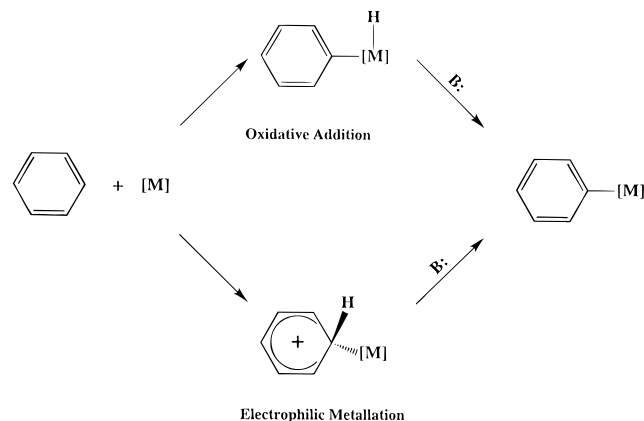
**Abstract:** Reaction of the ligand 1,3-bis((di-*tert*-butylphosphino)methyl)benzene (**1a**) with the [RhCO]<sup>+</sup> fragment in THF resulted in clean formation of the crystallographically characterized bis-chelated complex **2a** which contains an  $\eta^2$  agostic Rh C–H bond. Both the NMR data and the X-ray crystal structure show strong interaction between the metal center and the agostic C–H bond, which results in high acidity of the agostic proton. Reaction of **2a** with a weak organic base (NEt<sub>3</sub> or collidine) affords the known cyclometalated complex **3**. Reaction of the new ligand 1,3-bis((di-*tert*-butylphosphino)methyl)-4,5,6-trimethoxybenzene (**1b**) with the [RhCO]<sup>+</sup> fragment in THF gives the analogous to **2a** agostic complex **2b**. Analysis of the NMR data and the reactivity of both **2a** and **2b** showed that there is very little, if any, contribution of a metal arenium structure. This interpretation is supported by B3LYP/LANL2DZ density functional calculations on model compounds. Thus, deprotonation of  $\eta^2$  aromatic C–H agostic complexes can be proposed as an alternative route to electrophilic metalation of aromatic compounds.

## Introduction

Aromatic C–H activation by metal complexes is an area of much current interest.<sup>1</sup> One of the generally accepted mechanisms for metal-assisted inter- or intramolecular carbon–hydrogen bond cleavage involves a concerted metal insertion into this bond (oxidative addition) preceded by the formation of an  $\eta^2$  metal arene complex.<sup>2</sup> Another general mechanism is believed to proceed via an electrophilic attack at the ipso-carbon to form a metal arenium (Wheland) complex followed by proton elimination<sup>1d,3,4</sup> (Scheme 1). Surprisingly, despite this general belief, no such complex has ever been isolated in a reaction of a metal complex with an aromatic compound. Moreover, the kinetics of electrophilic metalation of arenes by transition metal complexes is not always reminiscent of aromatic electrophilic substitution. For example, the  $\rho$  values for this reaction are often substantially lower than those observed in organic S<sub>E</sub>Ar reactions and the regioselectivity with substituted aromatics does not always correspond to the expected pattern.<sup>1a</sup>

It had been suggested that in intramolecular processes the aromatic C–H bond activation might occur via an  $\eta^2$  C–H agostic intermediate or transition state,<sup>5</sup> although examples of

## Scheme 1



such complexes are exceedingly rare.<sup>6</sup> As no chemical properties have been reported, it is unclear whether this type of interaction results in increased acidity of the agostically bound proton, as has been observed in aliphatic agostic complexes.<sup>7</sup> If so, the increased acidity might lead to facile deprotonation of the arene to give the metalated product without actual metal insertion into the C–H bond, i.e., a process similar to electrophilic metalation.<sup>8</sup> Here we demonstrate that, using an ap-

(5) Lavin, M.; Holt, E. M.; Crabtree, R. H. *Organometallics* **1989**, *8*, 99.

(6) (a) Dani, P.; Karlen, T.; Gossage, R. A.; Smeets, W. J. J.; Spek, A. L.; van Koten, G. *J. Am. Chem. Soc.* **1997**, *119*, 11317. (b) Albeniz, A. C.; Schulte, G.; Crabtree, R. H. *Organometallics* **1992**, *11*, 242.

(7) Agostic metal complexes are normally viewed as intermediates (or transition states) toward C–H oxidative addition. For reviews, see: (a) Hall, C.; Perutz, R. N. *Chem. Rev.* **1996**, *96*, 3125. (b) Brookhart, M.; Green, M. L. H.; Wong, L.-L. *Prog. Inorg. Chem.* **1988**, *36*, 1. (c) Crabtree, R. H.; Hamilton, D. G. *Adv. Organomet. Chem.* **1988**, *28*, 299.

(8) Agostic interactions that do not lead to an increase in acidity and subsequent deprotonation of aromatic C–H bonds were reported: Perera, S. D.; Shaw, B. L. *J. Chem. Soc., Dalton Trans.* **1995**, 3861.

<sup>†</sup> Department of Organic Chemistry.

<sup>‡</sup> Department of Chemical Services.

(1) For recent reviews see: (a) Shilov, A. E.; Shul'pin, G. B. *Chem. Rev.* **1997**, *97*, 2879. (b) Crabtree, R. H. *Chem. Rev.* **1985**, *85*, 245. (c) Arndtsen, B. A.; Bergman, R. G.; Mobley, T. A.; Peterson, T. H. *Acc. Chem. Res.* **1995**, *28*, 154. (d) Taylor, R. *Electrophilic Aromatic Substitution*; John Wiley & Sons: New York, 1990; Chapter 5, p 173. (e) Sen, A. *Acc. Chem. Res.* **1988**, *21*, 421.

(2) (a) Jones, W. D.; Feher, F. J. *J. Am. Chem. Soc.* **1982**, *104*, 4240. (b) Jones, W. D.; Feher, F. J. *Acc. Chem. Res.* **1989**, *22*, 91.

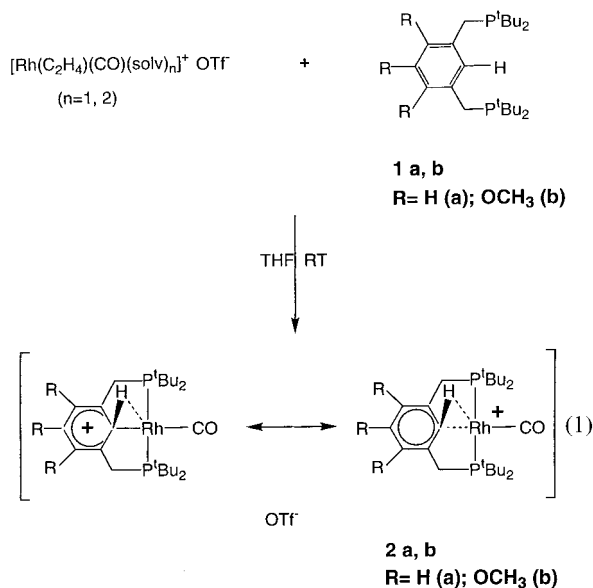
(3) For detailed studies on late transition metal complexes, see: (a) Aoyama, Y.; Yoshida, T.; Sakurai, K.; Ogoshi, H. *Organometallics* **1986**, *5*, 168. (b) Shul'pin, G. B.; Nizova, G. V.; Nikitaev, A. T. *J. Organomet. Chem.* **1984**, *276*, 115. (c) Sweet, J. R.; Graham, W. A. G. *J. Am. Chem. Soc.* **1983**, *105*, 305.

(4) For a review on cyclometalation, see: Ryabov, A. D. *Chem. Rev.* **1990**, *90*, 403.

appropriate metal precursor and ligand system, it is possible to isolate the *agostic intermediate* for the aromatic C–H cyclometalation process,<sup>7</sup> which can be easily deprotonated. Significantly, very little, if any, contribution from a metal arenium structure is observed. This provides an attractive alternative to the electrophilic aromatic substitution mechanism, which does not require a metal-stabilized arenium intermediate. Evidence for aromatic metalation by scandium complexes via a  $\sigma$ -bond metathesis mechanism without participation of the aromatic  $\pi$ -system was presented.<sup>9</sup>

## Results and Discussion

While studying the mechanisms of C–H and C–C bond activation in PCP-type ligands with various metals, we examined the reactivity of unsaturated, relatively *electron-poor* rhodium(I) precursors. Surprisingly, although various platinum group metals readily cyclometalate ligand **1a**, as first shown by Shaw and co-workers,<sup>10</sup> no C–H bond activation was observed when **1a** was treated with an equimolar amount of  $[\text{Rh}(\text{C}_2\text{H}_4)(\text{CO})(\text{solvent})_n]^+$  ( $n = 1, 2$ )<sup>11</sup> in THF. Rather, the reaction smoothly produced complex **2a** which contains an  $\eta^2$  C–H bond (eq 1). Complex **2a** is an air-stable compound and has been fully spectroscopically characterized including a single-crystal X-ray analysis.



The <sup>31</sup>P NMR spectrum of complex **2a** exhibits a doublet at 34.90 ppm ( $J_{\text{RhP}} = 100.4$  Hz). An important feature of the <sup>1</sup>H NMR spectrum of **2a** is the high-field shift of the proton attached to the ipso-carbon giving rise to a doublet at 4.13 ppm. However, the large value of the <sup>2</sup> $J_{\text{RhH}}$  coupling constant of 18.1 Hz suggests some sort of “agostic” interaction between the metal and this proton (vide infra). In the <sup>13</sup>C NMR spectrum of **2a** the ipso-carbon atom exhibits a signal at 110.95 ppm, which

**Table 1.** Selected Bond Lengths (Å) and Angles (deg) for **2a**

(a) Bond Lengths			
Rh(1)–C(1)	1.820 (5)	C(11)–C(12)	1.408 (8)
Rh(1)–C(11)	2.273 (5)	C(12)–C(13)	1.398 (7)
Rh(1)–H(11)	1.950	C(13)–C(14)	1.384 (8)
Rh(1)–P(2)	2.330 (2)	C(14)–C(15)	1.385 (8)
Rh(1)–P(3)	2.325 (2)	C(15)–C(16)	1.403 (7)
C(1)–O(1)	1.146 (6)	C(11)–C(16)	1.386 (9)
(b) Angles			
P(2)–Rh(1)–P(3)	167.32 (5)	Rh(1)–H(11)–C(11)	97.57
P(2)–Rh(1)–C(1)	96.2 (2)	Rh(1)–C(11)–H(11)	58.28
P(2)–Rh(1)–C(11)	83.9 (2)	C(12)–C(11)–C(16)	123.9 (5)
H(11)–Rh(1)–C(11)	24.15	C(12)–C(11)–Rh(1)	109.1 (3)

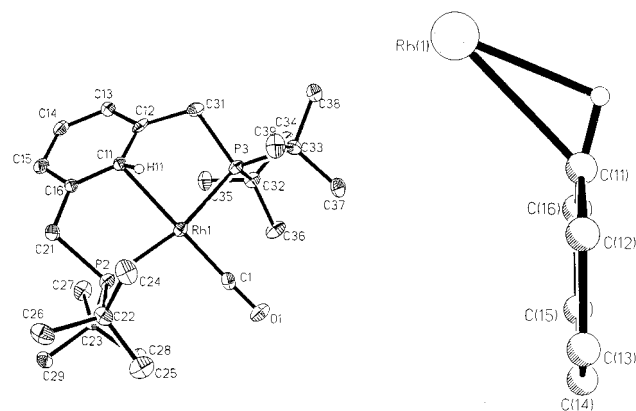


**Figure 1.** (a) ORTEP view of a molecule of **2a** with the thermal ellipsoids at 50% probability. The hydrogen atoms (except H(11)) are omitted for clarity. (b) Molecular view of a molecule of **2a** showing the mutual orientation of the aromatic ring and the metal center.

represents a large upfield shift relative to the ipso-carbon of cyclometalated PCP Rh complexes. Noteworthy, there is no observable coupling between the Rh atom and the ipso-C, which can be as large as 30 Hz in similar Rh(I) PCP systems,<sup>12</sup> indicating that the interaction between the two atoms is weak. We also note the relatively low <sup>1</sup> $J_{\text{HC}}$  coupling constant of 123 Hz, as compared to 163 and 165 Hz for the other two aromatic C–H bonds.<sup>13</sup>

Orange plates of **2a** suitable for X-ray analysis were obtained by slow crystallization of a  $\text{CH}_2\text{Cl}_2$  solution of **2a** at room temperature. Selected bond distances and bond angles are given in Table 1. The structure of **2a** clearly demonstrates (Figure 1) a strong metal interaction with the ipso-C–H bond, while the aromaticity of the ring remains practically intact. In good agreement with the <sup>13</sup>C NMR data, the distance between the ipso-carbon and the Rh atom is extremely long (2.273(5) Å) relative to regular rhodium–carbon  $\sigma$ -bonds and it is even longer than that in closely related Rh olefin complexes.<sup>14</sup> The rhodium–ipso-carbon bond length in neutral aromatic PCP complexes is normally substantially shorter (cf. 1.999(7) Å in  $\text{ClRh}(\text{H})[\text{C}_6\text{H}_3\text{-1,3-(CH}_2\text{P}(t\text{-Bu})_2)_2]$ <sup>15</sup> and 2.02(2) Å in  $\text{ClRh}(\text{CH}_3)[\text{C}_6\text{H}(\text{CH}_3)_2(\text{CH}_2\text{P}(t\text{-Bu})_2)_2]$ ,<sup>12a</sup> respectively). The carbon–carbon distances inside the ring are equal within the experimental error and are of values expected for aromatic compounds.

(9) Thompson, M. E.; Baxter, S. M.; Bulls, A. R.; Burger, B. J.; Nolan, M. C.; Santasiero, B. D.; Schaefer, W. P.; Bercaw, J. E. *J. Am. Chem. Soc.* **1987**, *109*, 203.

(10) Moulton, C. J.; Shaw, B. L. *J. Chem. Soc., Dalton. Trans.* **1976**, 1020.

(11) The complex  $[\text{Rh}(\text{C}_2\text{H}_4)(\text{CO})(\text{solvent})_n]^+$  ( $n = 1, 2$ ) was prepared in situ according to a general procedure reported in: (a) Schrock, R. R.; Osborn, J. A. *J. Am. Chem. Soc.* **1971**, *93*, 3089. The source was the known  $[\text{Rh}(\text{C}_2\text{H}_4)(\text{CO})\text{Cl}]_2$ ; (b) Powell, J.; Shaw, B. L. *J. Chem. Soc. A* **1968**, 211.

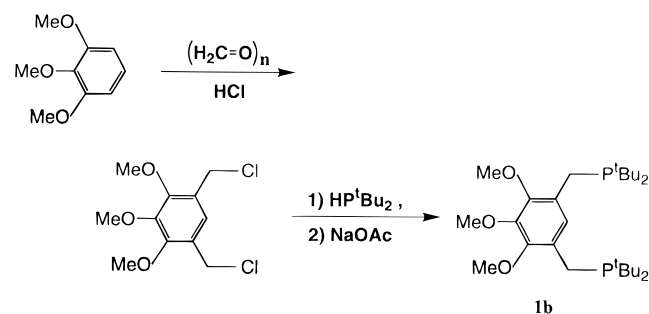
(12) (a) Rytchinski, B.; Vigalok, A.; Ben-David, Y.; Milstein, D. *J. Am. Chem. Soc.* **1996**, *118*, 12406. (b) Vigalok, A.; Ben-David, Y.; Milstein, D. *Organometallics* **1996**, *15*, 1838.

(13) Lowering of <sup>1</sup> $J_{\text{CH}}$  is often used as an indication for the presence of agostic interactions. See refs 7b,c for more details.

(14) (a) Vigalok, A.; Shimon, L. J. W.; Milstein, D. *J. Am. Chem. Soc.* **1998**, *120*, 477. (b) Vigalok, A.; Milstein, D. *J. Am. Chem. Soc.* **1997**, *119*, 7873.

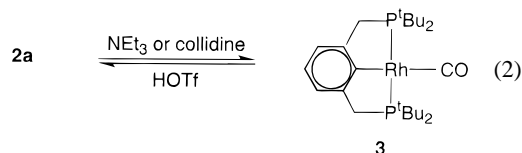
(15) Nemeš, S.; Jensen, C.; Binamira-Soriaga, E.; Kaska, W. C. *Organometallics* **1983**, *2*, 1442.

## Scheme 2



The H(11) atom (which was located independently) strongly interacts with the Rh(1) (1.950 Å), which was also evident from the  $^1\text{H}$  NMR spectrum of **2a**. It is noteworthy that this hydrogen is removed from the aromatic plane by ca.  $17^\circ$ , whereas the C–H bond length of 0.93 Å is in the range observed in X-ray diffraction measurements for unactivated hydrocarbons.<sup>16</sup> The calculated  $r_{\text{bp}}$  value of 0.73 is indicative of a very strong  $\eta^2$  C–H agostic interaction in **2a**.<sup>16</sup>

Although the X-ray structure of **2a** does not show noticeable distortion from aromaticity in the ring, the removal of the ipso-C–H bond from the plane suggests that the contribution of the arenium (Wheland type) form cannot be excluded. The agostic proton in **2a** is somewhat acidic, and it undergoes slow exchange with excess of  $\text{D}_2\text{O}$  (~30% conversion after 18 h at room temperature in THF). Moreover, the reaction with relatively weak bases such as  $\text{NEt}_3$  or collidine results in deprotonation of **2a** and formation of the known Rh(I) carbonyl complex  $\text{Rh}(\text{CO})[\text{C}_6\text{H}_3\text{-1,3-(CH}_2\text{P}(t\text{-Bu)}_2)_2]$ <sup>10</sup> (**3**). The reaction is reversed upon addition of HOTf (eq 2). While deprotonation of aliphatic



agostically bound protons is a known process,<sup>17</sup> it has not yet been demonstrated with aromatic hydrocarbons. In the latter, the HX elimination during metalation is solely attributed to the *electrophilic pathway*.<sup>1,3,18</sup> If **2a** is however viewed as an arenium species, then its thermodynamic stability is somewhat unexpected, as most of the protonated Wheland intermediates can be observed only at low temperatures and/or in the presence of excess of superacids.<sup>19</sup>

Obviously, the arenium form must be influenced by electron-donating or -withdrawing substituents on the ring. To explore a substituent effect, the new ligand **1b**, bearing three methoxy groups in the aromatic ring, was synthesized (Scheme 2). When **1b** was reacted with 0.5 equiv of  $[\text{Rh}(\text{COE})_2\text{Cl}]_2$  at room

(16) The real values of C–H bond distances are somewhat larger than those obtained from the X-ray studies. See, for example: Crabtree, R. H.; Holt, E. M.; Lavin, M.; Morehouse, S. M. *Inorg. Chem.* **1985**, *24*, 1986.

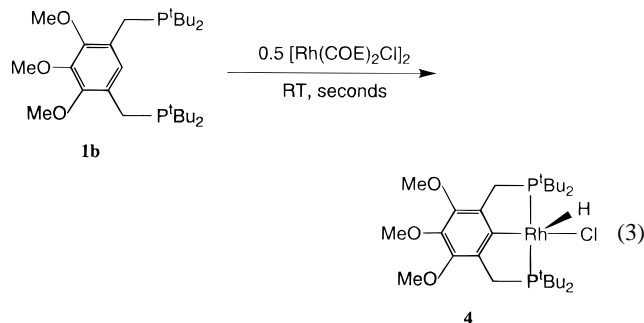
(17) (a) Speckman, D. M.; Knobler, C. B.; Hawthorne, M. F. *Organometallics* **1985**, *4*, 1692. (b) Kanamori, K.; Broderick, W. E.; Jordan, R. F.; Willett, R.; Legg, J. I. *J. Am. Chem. Soc.* **1986**, *108*, 7122.

(18) A reviewer suggested that deprotonation of **2a** can take place from an unobserved Rh(III) carbonyl hydride, which can be in equilibrium with the agostic **2a**. While an equilibrium involving fluxional rhodium hydride complexes of bis(di-*tert*-butylphosphino)pentane was reported in the following references, no evidence for such an equilibrium was obtained in our rigid system: (a) Crocker, C.; Errington, R. J.; Markham, R.; Moulton, C. J.; Shaw, B. L. *J. Chem. Soc., Dalton Trans.* **1982**, 387. (b) Crocker, C.; Errington, R. J.; Markham, R.; Moulton, C. J.; Odell, K. J.; Shaw, B. L. *J. Am. Chem. Soc.* **1980**, *102*, 4373. In addition, such an equilibrium cannot explain the deuteration of **2a** with  $\text{D}_2\text{O}$ .

**Table 2.** Comparative Analysis of Selected NMR Data (ppm) for Complexes **2a** and **2b** and for Parent Ligands **1a** and **1b**, Respectively ( $\text{CDCl}_3$ , 23 °C)

NMR signal	ligand vs complex					
	$\delta(\mathbf{1a})$	$\delta(\mathbf{2a})$	$\Delta\delta$	$\delta(\mathbf{1b})$	$\delta(\mathbf{2b})$	$\Delta\delta$
para-C	128.10	138.34	10.24	149.42	159.98	10.56
meta-C	126.60	127.62	1.02	146.09	148.90	2.81
ortho-C	141.24	154.17	12.93	129.23	144.57	15.34
ipso-C	130.63	110.95	-19.68	127.15	104.77	-22.38
ipso-H	7.25	4.13	-3.12	7.11	4.13	-2.98

temperature, rapid formation of the cyclometalated hydrido chloride Rh(III) complex **4** took place in a quantitative yield within a few seconds (eq 3). By contrast, reaction with  $[\text{Rh}(\text{COE})_2\text{Cl}]_2$



$(\text{C}_2\text{H}_4)(\text{CO})(\text{solvent})_n]^+$  ( $n = 1, 2$ ) in THF smoothly produced the agostic complex **2b** (eq 1). Significantly, only very small changes in the NMR spectra of **2b** were noted in comparison to those of **2a**. Similar to the case of **2a**, the agostic proton bound to the ipso-carbon in **2b** shows a doublet at 4.13 ppm ( $J_{\text{RhH}} = 17.6$  Hz) in the  $^1\text{H}$  NMR spectrum and the ipso-carbon lacks the  $^1J_{\text{RhC}}$  coupling and appears at 104.77 ppm as a triplet ( $J_{\text{PC}} = 4.4$  Hz) in the  $^{13}\text{C}$  NMR spectrum. Table 2 compares selected  $^{13}\text{C}$  chemical shifts of complexes **2a** and **2b** to those of the parent ligands **1a** and **1b**, respectively. Interestingly, the  $\Delta\delta$  between the complex and ligand signals is nearly identical for the two complexes, indicating that contribution of the arenium structure in **2a** and **2b** is similar and not large as compared with the neutral C–H aromatic agostic structure. Moreover, the H/D exchange of the agostic protons in both **2a** and **2b** with  $\text{D}_2\text{O}$  proceeded with comparable rates, as was detected by  $^{31}\text{P}$  NMR spectroscopy (Figure 2), showing that the substituents in the ring do not play a significant role in the acidity of the agostic proton.

Although the neutral  $[\text{RhCl}]$  fragment easily oxidatively adds the C–H bond in PCP-type ligands to give the corresponding Rh(III) hydrido chloride complexes, the cationic  $[\text{RhCO}]^+$  fragment is not sufficiently electron rich to insert into the C–H bond. Complex **2a** is invariably stable in the  $-60$  to  $+90$  °C temperature range. This stability is a result of the strong C–H agostic interaction with the cationic metal center.<sup>20</sup> This agostic

(19) (a) Koptyug, V. A. *Contemporary Problems in Carbonium Ion Chemistry III*; Topics in Current Chemistry 122; Springer-Verlag: Berlin, 1984. See also: (b) Brouwer, D. M.; Mackor, E. L.; MacLean, C. In *Carbonium Ions*; Olah, G. A., Schleyer, P. v. R., Eds.; Wiley: New York, 1970; Vol. 2, p 837. (c) Farcasiu, D. *Acc. Chem. Res.* **1982**, *15*, 46. (d) Farcasiu, D.; Marino, G.; Miller, G.; Kastrop, R. V. *J. Am. Chem. Soc.* **1989**, *111*, 7210. (e) Xu, T.; Barich, D. H.; Torres, P. D.; Haw, J. F. *J. Am. Chem. Soc.* **1997**, *119*, 406 and references therein.

(20) For recent examples of stabilizing agostic interactions in cationic late transition metal complexes with bulky phosphine ligands, see: (a) Huang, D.; Huffman, J. C.; Bolinger, J. C.; Eisenstein, O.; Caulton, K. G. *J. Am. Chem. Soc.* **1997**, *119*, 7398. (b) Cooper, A. C.; Streib, W. E.; Eisenstein, O.; Caulton, K. G. *J. Am. Chem. Soc.* **1997**, *119*, 9069. (c) Ujaque, G.; Cooper, A. C.; Maseras, F.; Eisenstein, O.; Caulton, K. G. *J. Am. Chem. Soc.* **1998**, *120*, 361.

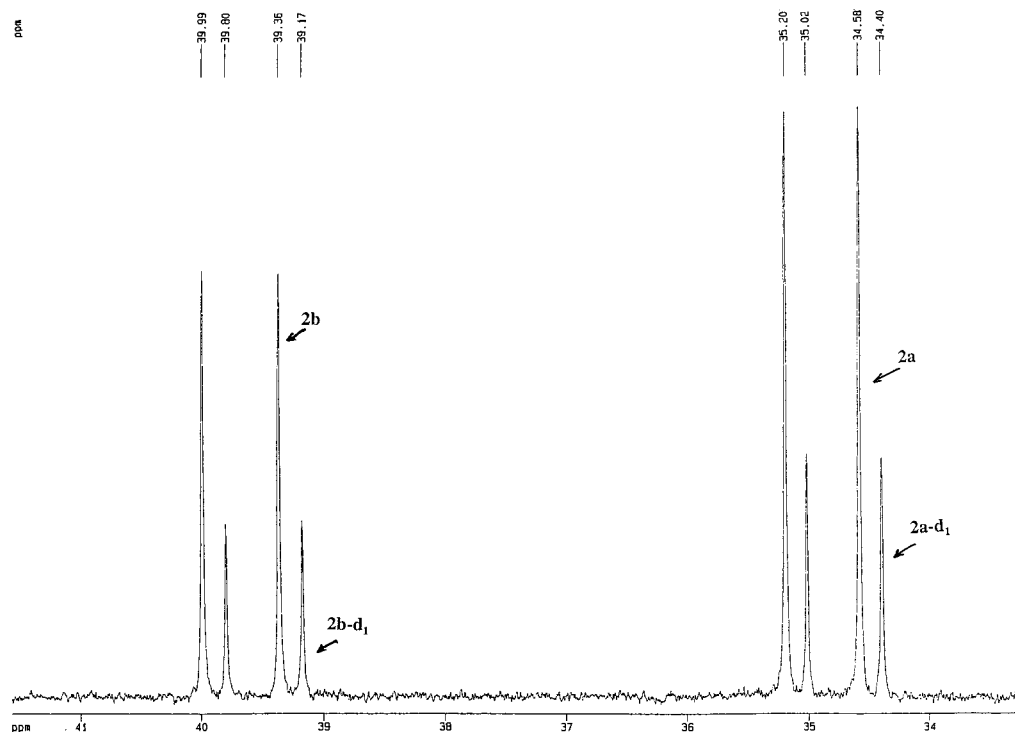
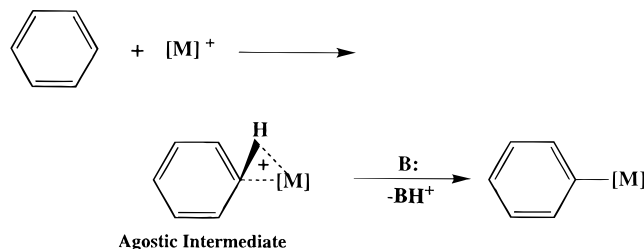


**Figure 2.**  $^{31}\text{P}\{^1\text{H}\}$  NMR spectrum ( $\text{CDCl}_3$ ) of the reaction of complexes **2a** (5 mg, 0.007 mmol) and **2b** (5 mg, 0.007 mmol) with  $\text{D}_2\text{O}$  (8  $\mu\text{L}$ , 0.400 mmol) in THF (1 mL) after 18 h at room temperature. Larger excesses of  $\text{D}_2\text{O}$  resulted in partial deprotonation of the complexes.

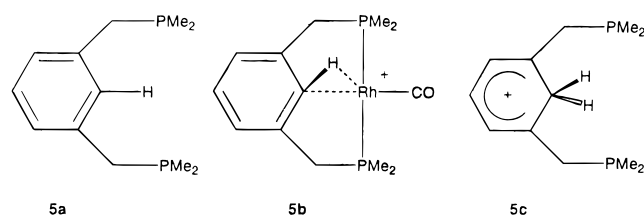
### Scheme 3



interaction results in increased acidity of the aromatic proton which can now be easily removed even by very weak bases. However, formal positive charge transfer from the metal to the aromatic ring to form an arenium-type species takes place, if at all, to only a minor extent. There are many instances of aromatic metalation where the oxidative addition and electrophilic mechanisms cannot be easily distinguished.<sup>21</sup> Thus, it is possible that metalation of aromatic hydrocarbons can occur via the formation and deprotonation of an  $\eta^2$  C–H agostic intermediate, the reactivity of which mimics the electrophilic activation mechanism (Scheme 3).

To further verify our interpretation, we have carried out B3LYP/LANL2DZ<sup>22–24</sup> density functional calculations on model compounds for **1a** and **2a** using Gaussian 94.<sup>25</sup> The model compounds, denoted **5a** and **5b** (Chart 1), respectively, solely differ by the substitution of smaller methyl groups for the *tert*-butyl groups. Our computed structure for **5b** agrees quite closely with the corresponding parts of the X-ray structure of **2a**, except for somewhat more realistic C–H bond distances and (because of the absence of the triflate counterion)  $C_s$  symmetry.

### Chart 1



A contour plot of the computed electron density of **5b** in the  $\text{C}_{\text{ipso}}\text{--H}_{\text{ipso}}\text{--Rh}$  plane is given in Figure 3. The picture of the electron density between the ipso-C–H bond and the Rh atom is strongly suggestive of an agostic interaction. Between the Rh and  $\text{C}_{\text{ipso}}$  atom, a Löwdin bond order<sup>26</sup> of 0.43 is found; that between Rh and  $\text{H}_{\text{ipso}}$  is only 0.13. As expected, the  $\text{C}_{\text{ipso}}\text{--H}_{\text{ipso}}$  bond is somewhat weakened by this interaction; the Löwdin bond order is 0.73 (compared to 0.87 for the other ring C–H bonds), while the computed  $\text{C}_{\text{ipso}}\text{--H}_{\text{ipso}}$  bond length is 0.026 Å longer than the other aromatic C–H bonds.

The calculations offer several gauges for arenium (Wheland) character. Relative to those of **5a**, the ring bond lengths in **5b** are affected only quite weakly:  $\text{C}_{\text{ipso}}\text{--C}_{\text{ortho}} +0.011$  Å,  $\text{C}_{\text{ortho}}\text{--C}_{\text{meta}} -0.007$  Å,  $\text{C}_{\text{meta}}\text{--C}_{\text{para}} -0.006$  Å. For comparison, the corresponding values for the arenium compound of **5a**, denoted **5c** here, at the same level of theory are +0.088, –0.019, and +0.009 Å. Noticeable alternation is seen in the Löwdin bond orders in the benzene ring of **5b**: ipso–ortho 1.33, ortho–meta 1.46, and meta–para 1.49, compared to 1.44, 1.43, and 1.50,

(21) See, for example: (a) Brainard, R. L.; Nutt, W. R.; Lee, T. R.; Whitesides, G. M. *Organometallics* **1988**, *7*, 2379. (b) Cordone, R.; Harman, W. D.; Taube, H. *J. Am. Chem. Soc.* **1989**, *111*, 2896.

(22) Becke, A. D. *J. Chem. Phys.* **1993**, *98*, 5648.

(23) Lee, C.; Yang, W.; Parr, R. G. *Phys. Rev. B* **1988**, *37*, 785.

(24) Hay, P. J.; Wadt, W. R. *J. Chem. Phys.* **1985**, *82*, 270, 284, 299.

(25) Frisch, M. J.; Trucks, G. W.; Schlegel, H. B.; Gill, P. M. W.; Johnson, B. G.; Robb, M. A.; Cheeseman, J. R.; Keith, T.; Petersson, G. A.; Montgomery, J. A.; Raghavachari, K.; Al-Laham, M. A.; Zakrzewski, V. G.; Ortiz, J. V.; Foresman, J. B.; Cioslowski, J.; Stefanov, B. B.; Nanayakkara, A.; Challacombe, M.; Peng, C. Y.; Ayala, P. Y.; Chen, W.; Wong, M. W.; Andres, J. L.; Replogle, E. S.; Gomperts, R.; Martin, R. L.; Fox, D. J.; Binkley, J. S.; Defrees, D. J.; Baker, J.; Stewart, J. P.; Head-Gordon, M.; Gonzalez, C.; Pople, J. A. *Gaussian 94*, Revision D.4; Gaussian, Inc.: Pittsburgh, PA, 1995.

(26) Natiello, M. A.; Medrano, J. A. *Chem. Phys. Lett.* **1984**, *105*, 180.



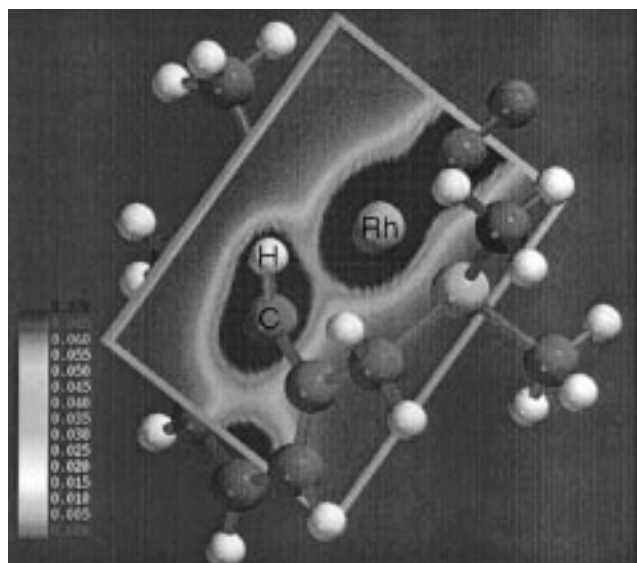


**Figure 3.** Plot of the B3LYP/LANL2DZ electron density in the  $C_{\text{ipso}}-H_{\text{ipso}}-Rh$  plane.

respectively, in **5a**. The alternation is however much smaller than in **5c** (1.10, 1.54, and 1.44, respectively).

The dihedral angle  $C_{\text{meta}}-C_{\text{ortho}}-C_{\text{ipso}}-H_{\text{ipso}}$  in **5b** differs from the ideal planar value ( $180^\circ$ ) by only  $16.3^\circ$ , compared to  $61.6$  and  $48.8^\circ$  for the two ipso hydrogens in **5c**. Furthermore, taking the difference between the NPA populations of  $[RhCO]^+$  and **5a** on one hand and **5b** on the other hand, we see that most of the positive charge remains concentrated on the Rh and particularly its  $-P(\text{alkyl})_2$  ligands, while the sum of all the charge differences on the non-ipso ring carbons is only 0.19, or 0.26 when the charges borne by their hydrogens are included in the total. In short, while we do have an arenium contribution, it is a very weak one, and an interpretation of **5b**, viz. **2a**, in terms of an agostic interaction rather than a Wheland complex certainly appears to be valid.

In conclusion, we have prepared and fully characterized novel chelated Rh(I) complexes with an  $\eta^2$  aromatic C–H agostic interaction. These complexes demonstrate relatively strong C–H acidity—so far unobserved for aromatic compounds—and they can be deprotonated by weak organic bases to give the corresponding cyclometalated products. The observed reactivity of these agostic complexes is similar to that attributed to metal arenium complexes—crucial intermediates in electrophilic aromatic metalation. However, the NMR data analysis and deuterium-labeling experiments have shown that there is very little, if any, contribution of a metal arenium structure in these molecules. This interpretation is supported by the computed electron density, bond orders, charge distributions, and bond distances obtained using B3LYP/LANL2DZ density functional calculations. Thus, strong agostic interaction between a metal center and an aromatic compound followed by deprotonation can be considered as an alternative to the generally expected electrophilic aromatic metalation involving arenium intermediates.

## Experimental Section

**General Procedures.** All operations with air- and moisture-sensitive compounds were performed in a nitrogen-filled glovebox (Vacuum Atmospheres with a MO-40 purifier). All solvents were reagent grade or better. Pentane, benzene, and THF were distilled over sodium/benzophenone ketyl. All solvents were degassed and stored under high-purity nitrogen after distillation. All deuterated solvents (Aldrich) were

stored under high-purity nitrogen on molecular sieves ( $3 \text{ \AA}$ ).  $[Rh(C_2H_4)(CO)Cl]_2$ ,<sup>11b</sup> **1a**,<sup>10</sup> and 4,6-dichloromethyl-1,2,3-trimethoxybenzene<sup>27</sup> were prepared according to literature procedures.

$^1H$ ,  $^{31}P$ , and  $^{13}C$  NMR spectra were recorded at 400, 162, and 100 MHz, respectively, using a Bruker AMX400 spectrometer.  $^1H$  and  $^{13}C$  chemical shifts are reported in ppm downfield from TMS and referenced to the residual solvent  $h_1$  (7.24 ppm chloroform-*d*, 7.15 ppm benzene-*d\_6*) and all-*d* solvent peaks (77.00 ppm chloroform, 128.00 ppm benzene), respectively.  $^{31}P$  chemical shifts are in ppm downfield from  $H_3PO_4$  and referenced to an external 85% phosphoric acid sample. All measurements were performed at  $21^\circ C$  unless otherwise specified.

Density functional calculations were carried out with the Gaussian 94<sup>26</sup> package running on a DEC Alpha 500 workstation, using the B3LYP<sup>22,23</sup> exchange-correlation functional and the LANL2DZ<sup>24</sup> basis set/relativistic effective core potential combination. An initial structure for a model compound of **2a** was generated by symmetrizing the X-ray structure of **2a** to  $C_s$ , substituting methyl groups in standard geometries for the *tert*-butyl groups, and manually adjusting the overly short X-ray C–H distances. The geometry of this compound was then fully optimized, as were (for comparison) structures of  $[RhCO]^+$  and of a model compound for **1a** generated by deleting the  $[RhCO]^+$  moiety from the model compound for **2a**. A cross section of the electron density in the  $C_{\text{ipso}}-H_{\text{ipso}}-Rh$  plane was generated using Spartan,<sup>28</sup> while charge distributions were obtained using the natural population analysis (NPA)<sup>29</sup> method and bond orders were obtained by the Löwdin<sup>26</sup> method.

**Preparation of a THF Solution of  $[Rh(C_2H_4)(CO)(\text{solv})_n]^+$  ( $n = 1, 2$ ).** To 0.5 mL of a THF solution of  $[Rh(\text{ethylene})(CO)Cl]_2$  (10 mg, 0.026 mmol) was added 14 mg of  $AgOTf$  (0.054 mmol) in 1 mL of THF. The mixture was allowed to remain in the dark for 30 min, after which the precipitate of  $AgCl$  (7 mg, 0.049 mmol) was filtered off. The resulting pale yellow solution was used for further reactions with **1a** and **1b**.

**Ligand 1a.** The full NMR data (including the  $^{13}C$  NMR) have not been previously reported.<sup>10</sup>

$^{31}P\{^1H\}$ NMR ( $\delta$ , ppm) ( $CDCl_3$ ): 34.22 (s).  $^1H$  NMR ( $\delta$ , ppm): 7.25 (br s, 1H, ipso-ArH), 7.12–7.13 (overlapped signals of *p*- and *o*-ArH, 3H), 2.81 (d,  $J_{HH} = 3.1$  Hz, 4H,  $CH_2P$ ), 1.10 (d,  $J_{PH} = 10.8$  Hz, 36H, *t*-Bu).  $^{13}C\{^1H\}$  NMR ( $\delta$ , ppm): 141.24 (br d,  $J_{PC} = 11.5$  Hz, *o*-Ar), 130.63 (t,  $J_{PC} = 7.5$  Hz, ipso-C), 128.10 (s, *p*-Ar), 126.60 (dd,  $J_{PC} = 9.3$  Hz,  $J_{PC} = 1.9$  Hz, *m*-Ar), 31.69 (d,  $J_{PC} = 21.9$  Hz,  $C(CH_3)_3$ ), 29.75 (d,  $J_{PC} = 12.9$  Hz,  $C(CH_3)_3$ ), 28.41 (d,  $J_{PC} = 23.1$  Hz,  $CH_2P$ ). The assignments were confirmed by  $^{13}C$  DEPT and  $^{13}C-^1H$  2D correlation experiments.

**Complex 2a.** (a) To a THF solution of  $[Rh(C_2H_4)(CO)(\text{solv})_n]^+$  ( $n = 1, 2$ ) was added 1 mL of a THF solution of **1a** (22 mg, 0.056 mmol). The resulting solution was allowed to stand for 1 h, concentrated in a vacuum (to ca. 50% of the volume), and then poured into 5 mL of pentane. The yellow precipitate was filtered off with a cotton pad, washed with pentane, and redissolved in  $CH_2Cl_2$ . Removal of the solvent in a vacuum gave pure **2a** (27 mg, 77%).

(b) To a  $CH_2Cl_2$  solution of  $(CO)Rh[C_6H_3-1,3-(CH_2P(*t*-Bu))_2]^{10}$  (**3**) was added 1.2 equiv of HOTf. The  $^{31}P$  NMR spectrum showed quantitative formation of **2a**.

$^{31}P\{^1H\}$ NMR ( $\delta$ , ppm) ( $CDCl_3$ ): 34.90 (d,  $J_{RHP} = 100.4$  Hz).  $^1H$  NMR ( $\delta$ , ppm): 7.63 (t,  $J_{HH} = 8.2$  Hz, 1H, *p*-ArH), 7.24 (d,  $J_{HH} = 8.2$  Hz, 2H, *m*-ArH), 4.13 (d,  $J_{RHH} = 18.1$  Hz, 1H, ipso-ArH), 3.60 (AB quart,  $J_{HH} = 16.3$  Hz, 4H,  $CH_2P$ ), 1.45 (vt,  $J_{PH} = 7.6$  Hz, 18H, *t*-Bu), 1.23 (vt,  $J_{PH} = 7.3$  Hz, 18H, *t*-Bu).  $^{13}C\{^1H\}$  NMR ( $\delta$ , ppm): 188.60 (dt,  $J_{RHC} = 90.5$  Hz,  $J_{PC} = 11.8$  Hz, RhCO), 154.17 (td,  $J_{PC} = 4.2$  Hz,  $J_{RHC} = 1.7$  Hz, *o*-Ar), 138.34 (br d, *p*-Ar), 127.62 (t,  $J_{PC} = 5.6$  Hz, *m*-Ar), 110.95 (t,  $J_{PC} = 4.4$  Hz, ipso-C), 37.37 (t,  $J_{PC} = 8.5$  Hz,  $C(CH_3)_3$ ), 35.11 (td,  $J_{PC} = 9.1$  Hz,  $J_{RHC} = 1.3$  Hz,  $C(CH_3)_3$ ), 29.95 (t,  $J_{PC} = 10.7$  Hz,  $CH_2P$ ), 29.76 (t,  $J_{PC} = 2.4$  Hz,  $C(CH_3)_3$ ), 29.00 (t,  $J_{PC}$

(27) Monte, A. P.; Waldman, S. R.; Marona-Lewicka, D.; Wainscott, D. B.; Nelson, D. L.; Sanders-Bush, E.; Nichols, D. E. *J. Med. Chem.* **1997**, *40*, 2997.

(28) *Spartan User's Guide*, Version 4.1; Wavefunction, Inc.: Irvine, CA, 1995.

(29) Reed, A. E.; Curtiss, L. A.; Weinhold, F. *Chem. Rev.* **1988**, *88*, 899.

= 2.8 Hz, C(CH<sub>3</sub>)<sub>3</sub>). IR (film): 1981 cm<sup>-1</sup> (s). Anal. Found (calc): C, 46.28 (46.57); H, 6.30 (6.01).

**Ligand 1b.** A mixture of di-*tert*-butylphosphine (10.440 g, 71.5 mmol) and 4,6-dichloromethyl-1,2,3-trimethoxybenzene<sup>27</sup> (7.55 g, 28.6 mmol) in acetone (75 mL) was refluxed with stirring under argon for 24 h, resulting in white crystals of the diphosphonium salt. The salt was isolated and washed with cold acetone and with pentane to remove unreacted starting material. The salt was then dissolved in 90 mL of distilled degassed water, and to the clear solution was added 30 g of NaOAc in 90 mL of distilled degassed water. The organic product was extracted twice with 200 mL of CH<sub>2</sub>Cl<sub>2</sub>, and the organic layer was separated from the mixture and dried over Na<sub>2</sub>SO<sub>4</sub>. The solvent was evaporated under vacuum to give the product which was contaminated with phosphine oxides. Purification by column chromatography (silica) afforded pure **1b** in 55% yield (7.6 g).

<sup>31</sup>P{<sup>1</sup>H}NMR (δ, ppm) (CDCl<sub>3</sub>) 31.41 (s). <sup>1</sup>H NMR (δ, ppm): 7.11 (br t, ipso-ArH), 3.85 (s, 6H, m-OCH<sub>3</sub>), 3.82 (s, 3H, p-OCH<sub>3</sub>), 2.74 (d, *J*<sub>PH</sub> = 3.3 Hz, 4H, CH<sub>2</sub>P), 1.12 (d, *J*<sub>PH</sub> = 10.7 Hz, 36H, *t*-Bu). <sup>13</sup>C{<sup>1</sup>H} NMR (δ, ppm): 149.42 (t, *J*<sub>PC</sub> = 2.2 Hz, p-Ar), 146.09 (s, m-Ar), 129.23 (d, *J*<sub>PC</sub> = 11.5 Hz, o-Ar), 127.15 (t, *J*<sub>PC</sub> = 10.32 Hz, ipso-C), 60.75 (s, m-OCH<sub>3</sub>), 60.51 (s, p-OCH<sub>3</sub>), 31.79 (d, *J*<sub>PC</sub> = 23.7 Hz, C(CH<sub>3</sub>)<sub>3</sub>), 29.71 (d, *J*<sub>PC</sub> = 13.2 Hz, C(CH<sub>3</sub>)<sub>3</sub>), 21.98 (d, *J*<sub>PC</sub> = 24.3 Hz, CH<sub>2</sub>P).

**Complex 2b.** Complex **2b** was prepared and purified analogously to **2a**.

<sup>31</sup>P{<sup>1</sup>H}NMR (δ, ppm) (CDCl<sub>3</sub>): 39.76 (d, *J*<sub>RhC</sub> = 101.5 Hz). <sup>1</sup>H NMR (δ, ppm): 4.13 (d, *J*<sub>RhH</sub> = 17.6 Hz, 1H, ipso-ArH), 3.91 (s, 3H, p-OCH<sub>3</sub>), 3.86 (s, 6H, m-OCH<sub>3</sub>), 3.56 (AB quart, *J*<sub>HH</sub> = 16.3 Hz, 4H, CH<sub>2</sub>P), 1.44 (vt, *J*<sub>PH</sub> = 7.6 Hz, 18H, *t*-Bu), 1.21 (vt, *J*<sub>PH</sub> = 7.3 Hz, 18H, *t*-Bu). <sup>13</sup>C{<sup>1</sup>H} NMR (δ, ppm): 189.10 (dt, *J*<sub>RhC</sub> = 89.1 Hz, *J*<sub>PC</sub> = 11.6 Hz, RhCO), 159.98 (br m, p-Ar), 148.90 (td, *J*<sub>PC</sub> = 5.1 Hz, *J*<sub>RhC</sub> = 0.9 Hz, m-Ar), 144.57 (td, *J*<sub>PC</sub> = 4.3 Hz, *J*<sub>RhC</sub> = 1.7 Hz, o-Ar), 104.77 (t, *J*<sub>PC</sub> = 4.4 Hz, ipso-C), 62.40 (s, m-OCH<sub>3</sub>), 60.69 (s, p-OCH<sub>3</sub>), 36.95 (td, *J*<sub>PC</sub> = 8.1 Hz, *J*<sub>RhC</sub> = 0.6 Hz, C(CH<sub>3</sub>)<sub>3</sub>), 35.14 (td, *J*<sub>PC</sub> = 9.1 Hz, *J*<sub>RhC</sub> = 1.3 Hz, C(CH<sub>3</sub>)<sub>3</sub>), 29.28 (t, *J*<sub>PC</sub> = 2.5 Hz, C(CH<sub>3</sub>)<sub>3</sub>), 28.99 (t, *J*<sub>PC</sub> = 2.8 Hz, C(CH<sub>3</sub>)<sub>3</sub>), 23.48 (t, *J*<sub>PC</sub> = 10.4 Hz, CH<sub>2</sub>P). IR (film): 1992 cm<sup>-1</sup> (s).

**Complex 4.** To a suspension of [Rh(COE)<sub>2</sub>Cl]<sub>2</sub> (15 mg, 0.02 mmol) in 1 mL of THF was added 1 mL of a THF solution of **1b** (20 mg, 0.041 mmol). The resulting yellow solution showed quantitative formation of **4** on the basis of <sup>31</sup>P NMR spectroscopy. The solvent was evaporated, and the resulting yellow solid was dried in a vacuum. Yield: 25 mg (98%).

<sup>31</sup>P{<sup>1</sup>H}NMR (δ, ppm) (CDCl<sub>3</sub>): 74.15 (d, *J*<sub>RhC</sub> = 114.3 Hz). <sup>1</sup>H NMR (δ, ppm): 3.85 (s, 3H, p-OCH<sub>3</sub>), 3.83 (s, 6H, m-OCH<sub>3</sub>), 3.14 (AB quart, *J*<sub>HH</sub> = 17.9 Hz, 4H, CH<sub>2</sub>P), 1.36 (m, 36H, 2 overlapped *t*-Bu), -27.96 (dt, *J*<sub>RhH</sub> = 52.0 Hz, *J*<sub>PH</sub> = 11.9 Hz, 1H, RhH). <sup>13</sup>C{<sup>1</sup>H} NMR (δ, ppm): 154.34 (br d, *J*<sub>RhC</sub> = 33.2 Hz, ipso-C), 147.20 (td, *J*<sub>PC</sub> = 8.2 Hz, *J*<sub>RhC</sub> = 2.0 Hz, m-Ar), 141.62 (s, p-Ar), 139.26 (td, *J*<sub>PC</sub> = 10.4 Hz, *J*<sub>RhC</sub> = 1.3 Hz, o-Ar), 60.51 (s, p-OCH<sub>3</sub>), 60.03 (s,

m-OCH<sub>3</sub>), 36.27 (t, *J*<sub>PC</sub> = 7.6 Hz, C(CH<sub>3</sub>)<sub>3</sub>), 34.58 (td, *J*<sub>PC</sub> = 8.9 Hz, *J*<sub>RhC</sub> = 1.4 Hz, C(CH<sub>3</sub>)<sub>3</sub>), 29.78 (t, *J*<sub>PC</sub> = 2.7 Hz, C(CH<sub>3</sub>)<sub>3</sub>), 29.38 (t, *J*<sub>PC</sub> = 2.5 Hz, C(CH<sub>3</sub>)<sub>3</sub>), 28.70 (td, *J*<sub>PC</sub> = 11.6 Hz, *J*<sub>RhC</sub> = 2.6 Hz, CH<sub>2</sub>P). Anal. Found (calc): C, 52.40 (52.05); H, 7.99 (8.09).

**X-ray Analysis of the Structure of 2a.** Complex **2a** was crystallized from CH<sub>2</sub>Cl<sub>2</sub> at room temperature to give orange crystals. Crystal data: C<sub>26</sub>H<sub>44</sub>F<sub>3</sub>O<sub>4</sub>P<sub>2</sub>RhS, orange prism, 0.3 × 0.3 × 0.3 mm<sup>3</sup>, monoclinic, *P*2<sub>1</sub>/*c*, *a* = 8.510(2) Å, *b* = 23.825(5) Å, *c* = 14.801(3) Å, β = 93.97(3)° from 25 reflections, *T* = 110 K, *V* = 2993.7(11) Å<sup>3</sup>, *Z* = 4, *fw* = 674.52, *D<sub>c</sub>* = 1.497 Mg/m<sup>3</sup>, μ = 0.795 mm<sup>-1</sup>. Data collection and treatment: Rigaku AFC5R four-circle diffractometer, Mo Kα, graphite monochromator (λ = 0.710 73 Å), 5107 reflections collected, 1.62° ≤ θ ≤ 27.49°, 0 ≤ *h* ≤ 11, -2 ≤ *k* ≤ 16, -17 ≤ *l* ≤ 17, ω scan method, scan width 1.4°, scan speed 2°/min, typical half-height peak width 0.25°, 3 standards collected 27 times each, with a 6% change in intensity, 4764 independent reflections (*R*<sub>int</sub> = 0.0325). Solution and refinement: The structure was solved by the Patterson method (SHELXS-96). Full-matrix least-squares refinement was based on *F*<sup>2</sup> (SHELXL-93). Idealized hydrogens were placed and refined in a riding mode, with the exception of H(11) on C(11), which was located independently and refined freely; 345 parameters with no restraints; final *R*<sub>1</sub> = 0.0492 (based on *F*<sup>2</sup>) for data with *I* > 2σ(*I*) and *R*<sub>1</sub> = 0.0743 for all data based on all 4759 reflections; goodness-of-fit on *F*<sup>2</sup> = 1.015; largest electron density = 0.878 e/Å<sup>-3</sup>.

**Acknowledgment.** This work was supported by the Israel Science Foundation, Jerusalem, Israel, and by the MINERVA Foundation, Munich, Germany. The authors thank B. Rybtchinski for valuable discussions. D.M. is the holder of the Israel Matz Professorial Chair of Organic Chemistry. J.M.L.M. is a Yigal Allon Fellow, an Honorary Research Associate ("Onderzoekslider in Eremandaat") of the National Science Foundation of Belgium (NFWO/FNRS), and the Incumbent of the Helen and Milton A. Kimmelman Career Development Chair. O.U. participates in the Franco-Israeli Scientific Cooperation Program sponsored by the French Embassy in Israel.

**Supporting Information Available:** Text describing the crystal structure determination of **2a**, an ORTEP diagram of **2a**, tables of crystal data and structure refinement details, atomic coordinates, bond lengths and angles, anisotropic displacement parameters, and hydrogen atom coordinates for complex **2a**, and a table giving the B3LYP/LANL2DZ computed structures of **5a-c** in Cartesian coordinates (Å) (11 pages, print/PDF). See any current masthead page for ordering information and Web access instructions.

JA982534U